Supercritical Fluid Desorption Studies for Recovery of α-Caprolactam from Granular Activated Carbon after Wastewater Treatment: Modelling of Diffusive Behaviour

B. Al-Duri* and C.S. Kalpage
Dept of Chemical Engineering, School of Engineering, University of Birmingham, Edgbaston – Birmingham B15 2TT, UK. FAX: +(44)(121)(4145324), Email: B.Al-Duri@bham.ac.uk

This work investigated the recovery of Caprolactam from granular activated carbon (GAC-F400) by supercritical fluid desorption using CO_2 as solvent. The experimental section consisted of laboratory scale adsorption, solubility studies, and desorption rate. Theoretically, several mathematical models were applied to predict the diffusive behaviour in the system. Solubility studies in $scCO_2$ using semi-continuous system showed promising results and were successfully modelled by the Chrastil equation. Regeneration of Caprolactam-laden GAC-F400 was investigated as function of temperature, pressure, fluid flow rate, GAC particle size, and initial carbon loading. As expected, regeneration efficiency (RE) was found to be greatly dependent on the operating conditions. The use of ethanol as co-solvent was tested, and proved to greatly improve solubility. Desorption kinetic data were fitted to six mass transfer models with different assumptions regarding equilibrium behaviour and diffusive mode.

1. INTRODUCTION

Caprolactam is the principal raw material of nylon 6, a versatile compound used in numerous applications, mainly as fibres for industrial yarns, floor coverings and carpets as well as for engineering plastics and films. The Global Caprolactam production capacity was 2.1m MT in 2001, predicted to rise to 3.9m MT by the end of 2005. Caprolactam is hazardous air pollutant with acute dermatological effects, which can extend to chronic neurological, gastrointestinal, cardiovascular and immunological changes upon regular exposure, the reason why the NIOSH* and ACGIH** limited the maximum safe concentration to 1 mg/m^3 of Caprolactam vapour and dust for an 8 to 10-hour working day. For higher concentrations (up to 46 mg/m^3 vapour and 3 mg/m^3 dust) exposure is limited to 15 minutes.

Wastewaters produced by Caprolactam manufacturing plants contain about 5-10% Caprolactam, resulting in high alkalinity, salinity and COD value, apart from adverse economy. Biological treatment methods proved successful [1], however they do not achieve Caprolactam recovery, the reason why the current technology namely adsorption, followed by regeneration is suggested.

There is always a growing demand for GAC in wastewater treatment due to its superior adsorptive capacity dictated by its high porosity, surface area and abundant adsorption surface functional groups. Its comparatively high price (~ €50 per kg) necessitates regeneration for re-use. Of the existing techniques are thermal, chemical, biological and extractive (solvent) regeneration, of which SCF regeneration is the subject of this script. It offers more favourable properties than organic solvent regeneration due to the tuneable solubility, improved mass transfer properties, intact product and adsorbent. Further, it was put forward as a suitable process for industrial scale operation [2]. The present work

* National Institute of Occupational Safety and Health, USA.
** American Conference of Governmental Industrial Hygienists

investigates several experimental and theoretical aspects of GAC regeneration and Caprolactam recovery by $scCO_2$.

2. MATERIALS AND METHODS

2.1 Materials: Caprolactam ($(C_6H_{11}ON)$ was supplied by Sigma Chemicals UK, while GAC-Filtrasorb 400 was supplied by Chemviron carbon, UK Ltd. CO_2 of commercial grade was supplied by BOC Ltd.

2.2 The experimental rig: Figure 1 shows a schematic diagram of the experimental rig, which has been previously described by the author [3].

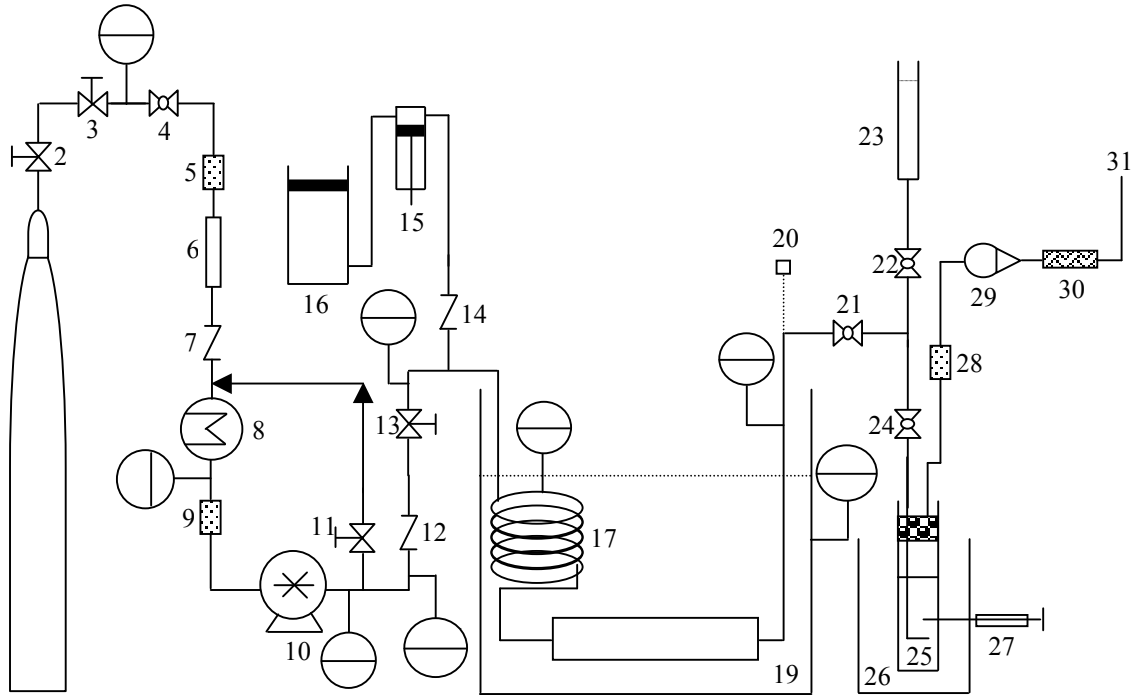

1. CO_2 cylinder; 2, 13. Stop valves; 3. Emergency shut-off valve; 4, 21. Ball valves; 5, 9, 28. On-line filters; 6. Drying tube; 7, 12, 14. Non-return valves; 8. Cooler/Heat exchanger; 10. Air driven liquid pump; 11. Back pressure regulator; 15. HPLC pump; 16. Co-solvent reservoir; 17. Coil heater; 18. Desorption column; 19. Water bath; 20. Bursting disc; 22. Gate valve; 23. Solvent reservoir; 24. Heated metering valve; 25. Cold trap; 26. Ice bath; 27. Sampling syringe; 28. Filter; 29. Rotameter; 30. Dry test meter; 31. Gas exit.

Figure 1: Schematic diagram of the experimental regenerating rig.

3. RESULTS AND DISCUSSION

3.1 Solubility studies:

Solubility of powdered Caprolactam was experimentally determined experimentally over the temperature and pressure ranges of 40 - 60ºC and 100 – 200 bars respectively. Being a small ring (Mol. Wt. = 113.6 g/mole) with a weekly polar lactam functional group, caprolactam showed good solubility in $scCO_2$. Figure 2 expectedly shows that the solubility increased with pressure and decreased with temperature.

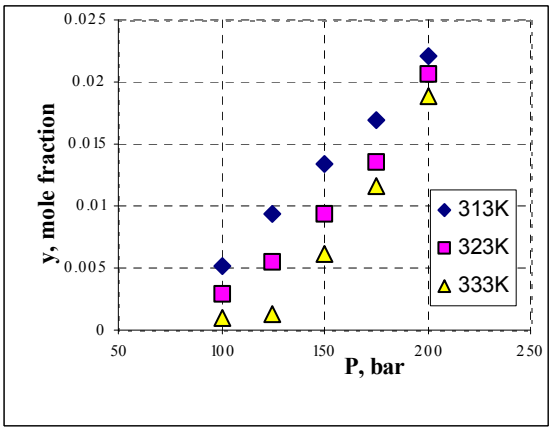

Figure 2: Experimental solubility data.

Higher pressures would increase the density and promote solvent-solute interactions and hence solubility, while higher temperatures (at constant pressure) mean lower density and solubility. As Caprolactam is in powder form it would require higher pressures (than 200 bars) for its vapour pressure to significantly aid solubility at higher temperatures. Theoretically, solubility data was successfully modelled by the Chrastil equation of [ln C = -75.524 + 11.967 ln ρ] where C and ρ are the solubility (g/L) and the SCF density, respectively.

3.2 Regeneration studies:

GAC-F400 regeneration by desorption was conducted as function of temperature (25-70ºC), pressure (80-285 bars), CO_2 flow rate (1-5 mL min^{-1}, at room temperature), GAC particle size (266-1190 µm), and the use of co-solvent. Apart from the other process parameters in conventional systems, solvent properties play a significant role in desorption in SCF systems.

3.2.1 Effects of Pressure and temperature:

Figures 3a and 3b show the effects of pressure upon the rate of desorption and amount adsorbed at 25ºC and 40ºC, respectively. As expected the rate and amount desorbed both increased with pressure due to the density increase. However, at 40ºC (and above) the system is more sensitive to pressure changes, the reason why desorption curves are more

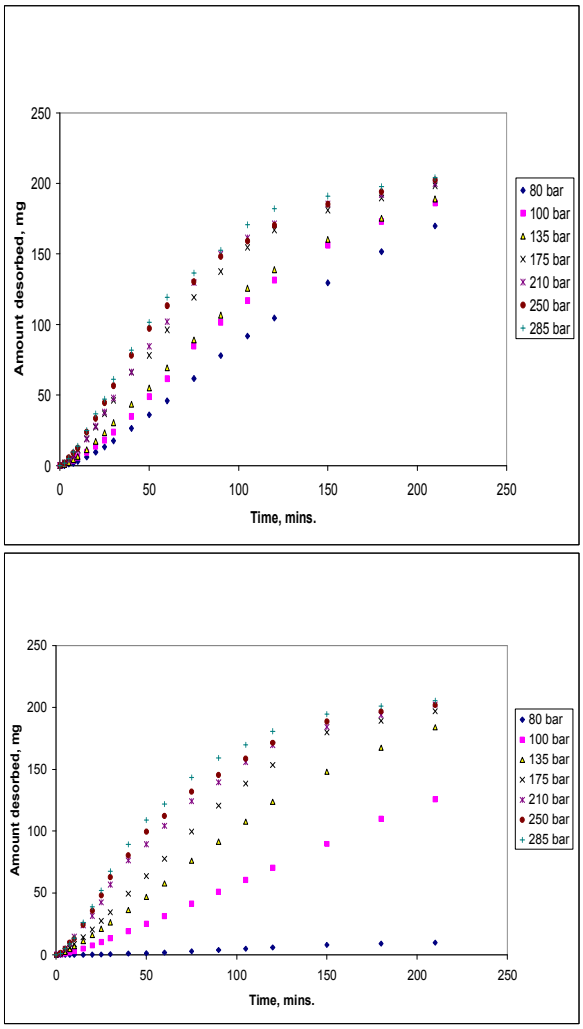

Figure 3: Effects of pressure on the desorption rate at (a) 25ºC and (b) 40ºC.

'spread-out' in Figure 3b, the factor that makes SC systems "tuneable" to the desired output. Carrying out regeneration studies up to 285 bars, the "cross over" pressure was observed around 220 bars, where the enhancement of solute vapour pressure overtook the reduction in density at higher temperatures. Above 220 bars, the process would favour higher temperatures and pressures [4, 5].

It is important to note that desorption rate and amount is not only controlled by the solubility of solute in CO_2. de Filippi *et al.*[6] found that despite comparable solubilities of atrazine and carbaryl in CO_2, atrazine- and carbaryl-loaded GACs were regenerated with 64% and 37.5% efficiency, respectively. The poly-disperse porous structure of GAC

highly affects the diffusive behaviour in the system and solute desorption, resulting in a non-linear desorption curve. In addition to the chemical properties of the adsorbate and its diffusive behaviour, the equilibrium behaviour of the Caprolactam/GAC system is an important factor, which would not exist in extraction processes. Adsorption isotherms of the current system [7] showed Langmuir irreversible behaviour. Even at the most favourable conditions, desorption efficiency was around 80%. This would be considered successful in terms of regeneration, yet the various effective factors *must be considered*. Upon mathematical modelling, adsorption isotherms would be considered, in addition to diffusion and continuity equations.

3.2.2 Effect of GAC particle size: In solid-fluid systems it is known that the particle size d_p is directly linked to diffusive behaviour.

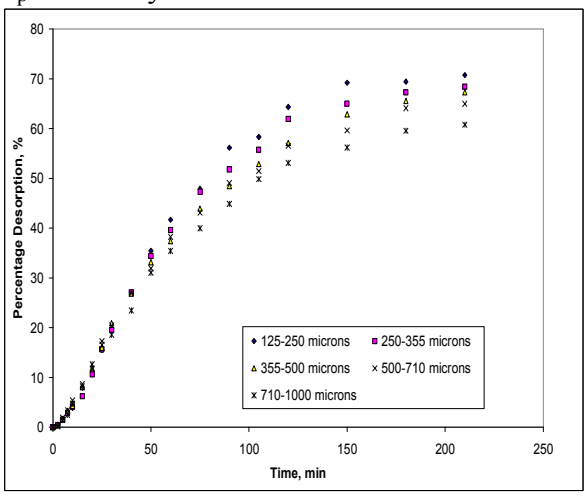

Figure 4: Desorption kinetics as function of GAC particle size.

Figure 4 shows that for the first hour, the rate and % desorption was not greatly influenced by d_p change as the process was mainly controlled by external mass transfer resistance and solubility. As intraparticle resistance was a prominent factor at later stages, d_p effect became apparent as larger particles have less accessible surface area and longer diffusion paths to the micropores where solute would be expected to reside.

3.2.3 Effect of CO_2 flow rate: Figure 5 shows that desorption rate expectedly increased with CO_2 flow due to improved diffusivity in high flow systems. However, % desorption rather depends on *total mass flow* as Figure 6 shows. Hence, upon design the CO_2 flow would be decided subject to factors other than the rate.

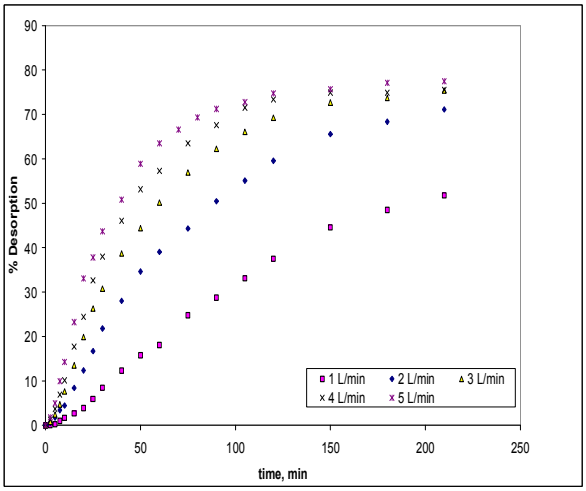

Figure5: % desorption versus time, at various CO_2 flow rates.

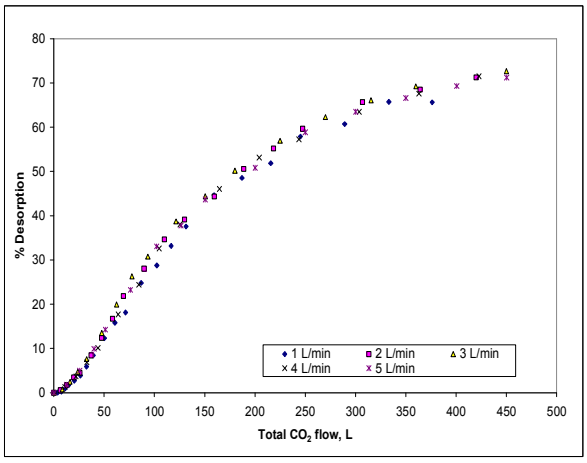

Figure 6: % desorption as function of total mass flow of CO_2, at various CO_2 flow rates.

3.2.4 Modelling Studies:

Generally, modelling of desorption considered the following: (1) film-transfer between the fluid bulk and particles, (2) intraparticle diffusion, (3) continuity (material balance) around the desorption bed, (4) dissociation (desorption rate kinetics), and (5) equilibrium isotherms. Detailed

equations can be found elsewhere [8, 7], so the main general equations are given below:

$$-E\frac{\partial^2 C}{\partial z^2}+\beta v\frac{\partial C}{\partial z}+\beta\frac{\partial C}{\partial t}+\frac{3k_f(1-\beta)}{r_0}\left\{C-(C_i)_{r=r_0}\right\}=0 \quad (1)$$

$$\varepsilon\frac{\partial C_S}{\partial t}=D_e\frac{1}{r^2}\frac{\partial}{\partial r}\left(r^2\frac{\partial C_i}{\partial r}\right)-\rho\frac{\partial q}{\partial t} \quad (2)$$

$$\frac{\partial q}{\partial t}=k_a(q_m-q)C_i-k_d q \quad (3)$$

Where E is the axial dispersion coefficient (m^2/s), D_e is the effective diffusivity within particles (m^2/s), k_f is the external mass transfer coefficient (m/s), k_a is the 2nd order adsorption coefficient (m^6/kmol s kg), k_d is the 1st order desorption rate constant (L/s), C is the concentration of solute in the fluid bulk (kmol/m^3), C_i is the solute concentration in the pore fluid, q is the solid phase concentration (kmol/kg), q_m is the equilibrium solid phase concentration (kmol/kg), v is the superficial velocity at the operating conditions (m/s), β is the bed voidage, ε is the particle porosity, ρ is the particle density (kg/m^3), t is the time (s), z is the bed length (m), r is the radial coordinate (m), and r_0 is the particle radius. For mathematical convenience the above general model was simplified in terms of one or more of the following: (i) mass transfer resistance and diffusive behaviour, (ii) desorption kinetic behaviour, and (iii) equilibrium behaviour; resulting in the models presented in this work:

3.2.4(a) Plug Flow Model: It assumes negligible axial dispersion, negligible intraparticle resistance, irreversible desorption and first order desorption kinetics. Hence Eq. (1) simplifies to:

$$v\frac{\partial C}{\partial z}+\frac{\partial C}{\partial t}+\left(\frac{1-\beta}{\beta}\right)\frac{3k_f}{r_0}\left\{C-(C_i)_{r=r_0}\right\}=0 \quad (4)$$

3.2.4(b) Recasens Models: They are based on parabolic solute concentration profile, linear resistance where both external mass transfer and intraparticle diffusivity are combined in a single overall mass transfer coefficient:

$$k_p=\frac{5k_f}{\left(5+\frac{k_f r_0}{D_e}\right)} \quad (5)$$

Hence desorption is controlled by a single averaged mass transfer resistance and dissociation rate. The latter was described in two different approaches: *Recasens model I* assumed linear dissociation (desorption) behaviour where Eq. (3) would be $q=KC$, while *Recasens model II* assumed irreversible dissociation where $\delta q/\delta t = k_d\, q$. *Recasens model III* combines the two with empirical approach.

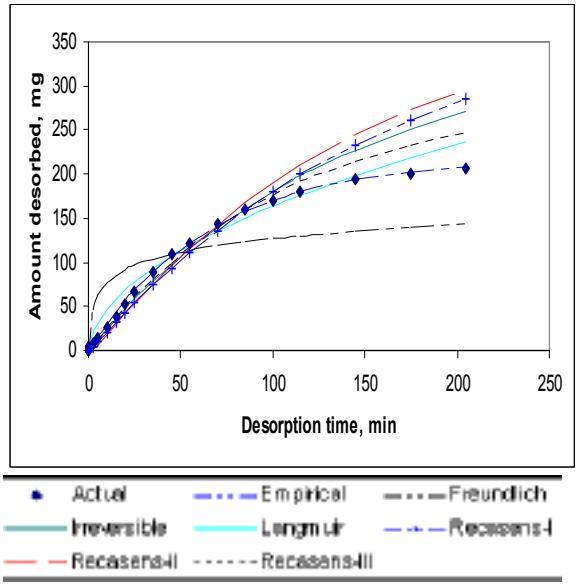

Fig 7: Application of mass transfer models to caprolactam desorption at 40°C and 285 bars, d_p = 520 µm.

3.2.4(c) Local Equilibrium Models: In these models desorption is assumed to be controlled by a local sorption isotherm, and it further assumes that there is absolutely no resistance to mass transfer internally or externally in particles. The behaviour of packed bed adorbers for low solute concentration loading was given by Ruthven [9] . The main assumptions in Eq. (4) are assumed to be valid in this model. Hence Eq. (4) is coupled with equilibrium isotherm

given in general form ($q^* = f(C)$) to provide Eq. (6):

$$\left(\frac{\partial z}{\partial t}\right)_c = \frac{u}{1+\left(\frac{1-\beta}{\beta}\right)\frac{dq^*}{dC}} \quad (6)$$

Where q^* is the equilibrium solid phase concentration. Eq. (6) can be rearranged and solved at $z = L$, (where L is the bed length) for appropriate sorption equilibriums.

$$t = \frac{L}{u}\left\{1+\left(\frac{1-\beta}{\beta}\right)\frac{dq^*}{dC}\right\} \quad (7)$$

Hence, q^* can be defined by the Langmuir or Freundlich isotherms. Figures 7 and 8 are sample results of the application of the various models. Clearly the Local Equilibrium Models show the poorest fit, due to neglecting mass transfer effects. Table 1 shows some calculations of the mass transfer parameters in some models at different d_p. The general trend shows mass transfer

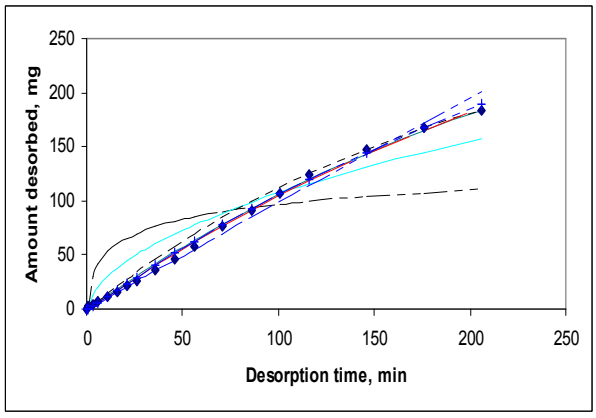

Figure 8: Application of mass transfer models at 40°C, 175 bars, d_p = 520 µm.

coefficient k_p to slightly decrease with d_p increase, and the equilibrium constant K decreases, showing reduced capacity with increased d_p.

Model	Parameter	Mean Particle Diameter, µm				
		265.7	437.9	520.6	760.9	1190.4
Recasens I	k_p x 10^8, m/s	6.1	6.0	5.9	5.7	5.2
	Kx10^3, m^3/kg	9.7	6.5	5.7	3.9	2.5
Recasens III	k_p x 10^7, m/s	2.2	2.2	2.2	2.1	2.0
	Kx10^2, m^2/kg	2.1	1.2	1.0	0.7	0.4
Irreversible	k_fx10^5, s^{-1}	10.6	10	9.6	7.9	7.2
Freundlich	Kx10^{-4}(m^3/kg)$^{1/n}$	8.5	8.5	8.5	8.5	8.4
	n x 10^{-4}	1.5	1.6	1.6	1.5	1.7

4. CONCLUSIONS

This work showed the diffusive behaviour in a supercritical desorption system, and illustrated the various operating system conditions and parameters that influence the overall performance of the desopber. Several mass transfer models were presented.

5. REFERENCES

[1] LEE, C.M., WANG, C.C., Water science and Technology, Vol 49, **2004**, p.341.

[2] McHUGH, M., & KRUKONIS, V., **1994**, Supercritical fluid extraction, 2nd edition. Butterworth-Heinemann.

[3] AL-DURI, B., KALPAGE, C.S., ISASF 9, **2004**, p.

[4] TAN, C.S., LIOU, D.C., Eng. Chem. Res., vol. 27 (7) **1988**, p.988.

[5] SIRINIVASAN, M.P., SMITH, J.M., McCOY, B.J. Chem. Eng. Sci., vol. 45 (7), **1990,** p. 1885.

[6] deFILIPPI, R.P., KRUKONIS, V.J., ROBEY, R.J., MODELL, M., E.P.A.Report 600/2-80-504, **1980.**

[7]KALPAGE, C.S., PhD thesis, University of Birmingham, **2005**.

[8] RECASENS, F., McCOY, B.J., SMITH, J.M., AIChE Journal, VOL. 35 (6), **1989**, p. 951.

[9] RUTHVEN, M.D., Principles of adsorption and adsorption processes, **1984**. John Wiley & Sons, Inc., USA.